CVEL

THE CLEMSON UNIVERSITY VEHICULAR ELECTRONICS LABORATORY

TECHNICAL REPORT: CVEL-14-055

Modeling the Conversion between Differential Mode and Common Mode Propagation in Transmission Lines

Li Niu and Dr. Todd Hubing

Clemson University

March 1, 2015

Contents

Abstract

When modeling differential signal propagation in a two-conductor transmission line over ground, it is convenient to express the propagation as the sum of two orthogonal modes, common-mode and differential mode. These TEM modes propagate independently as long as there is no change in the electrical balance of the three-conductor configuration. Any change in the electrical balance results in an exchange of power between the two modes at the point of the discontinuity. This effect can be precisely modeled using simple load resistances and dependent sources.

1. Introduction

High-speed digital signals are often transmitted from one point to another as differential signals on balanced two-conductor transmission lines. The balanced conductors generally have identical cross-sections and have the same electrical impedance to any other conductors in the system. In order to help maintain constant impedances, these two conductors are often located near a third reference conductor, typically labeled "ground". The differential-mode (DM) currents on the two signal conductors are equal in magnitude and flow in opposite directions everywhere along the transmission line. No current is intended to flow on the reference conductor; but discontinuities in the electrical balance of the two-conductor transmission line can cause energy to be converted from the differential-mode to common-mode (CM) reducing the amount of signal power available at the far end of the line and potentially contributing to unwanted coupling between the signal path and electrical noise.

Differential mode and common mode, also referred to as odd mode and even mode, propagation in TLs have been studied extensively. In [1]-[8], these modes of propagation were evaluated using multi-conductor transmission line theory. In [9]-[13], changes in transmission line impedances were viewed from the standpoint of introducing imbalance to an otherwise balanced transmission line. These papers modeled the coupling using ideal sources inserted in a modal equivalent circuit. In [13], the model was extended to include a complete description of the power flow within and between model equivalent circuits.

The concept of mode conversion due to changes in electrical balance has also been applied to the modeling of radiated emissions problems, where the common-mode currents do not return on a nearby conductor and the common-mode propagation is not TEM (e.g. [14]-[20]). However, the focus of this paper is modeling TEM mode conversion. Simple equivalent sources and loads are developed to model TEM mode conversion in terms of changes in electrical balance. The resulting models are generally simpler and more intuitive than models based on multi-conductor transmission line equations and can be applied whether the mode coupling is weak or strong.

2. Definition of Differential Mode and Common Mode Signals

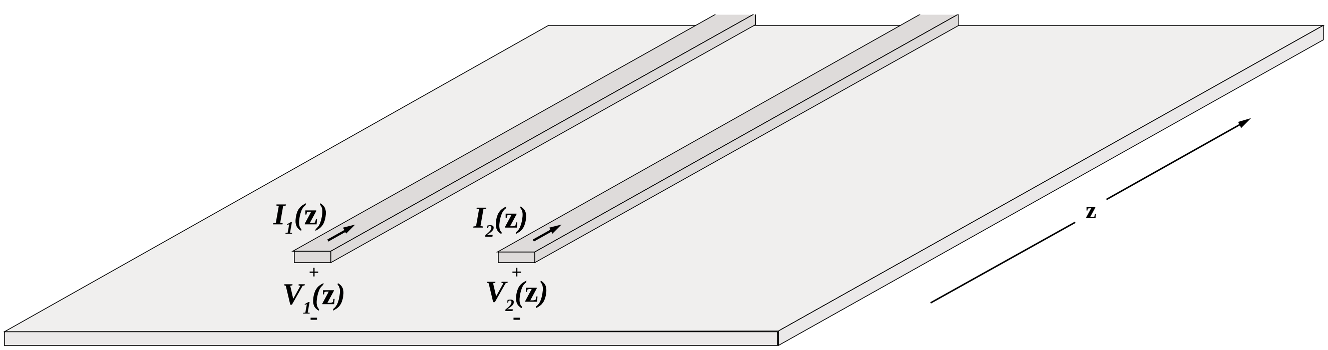

Fig. 1. A two-conductor TL above a reference plane.

Consider the pair of wires routed above a reference plane illustrated in Fig. 1. The currents on conductors 1 and 2 are $I_1(z)$ and $I_2(z)$, respectively. $V_1(z)$ and $V_2(z)$ are the voltages between each conductor and the reference plane.

If a signal is propagating differentially on the wire pair, it is inconvenient to view the propagation in terms of V_1, I_1 and V_2, I_2. Instead, it is preferable to express the propagation in terms of the two orthogonal modes of propagation modes typically referred to as differential mode (DM) and common mode (CM). These modes of propagation are associated with well-defined propagating voltages and currents, V_{DM}, I_{DM} and V_{CM}, I_{CM}. For a TEM wave propagating along the transmission line in the positive z-direction, we define the DM voltage as the voltage difference between two conductors,

$$V_{DM}^{+} = V_1^{+} - V_2^{+} \ . \tag{1}$$

The CM current is defined as the total current that flows on both conductors,

$$I_{CM}^{+} = I_1^{+} + I_2^{+} . \tag{2}$$

Since DM and CM are mutually independent, the voltage and current associated with each mode are related by their own characteristic impedances,

$$V_{DM}^{+} = Z_{DM} \cdot I_{DM}^{+} \ , \tag{3}$$

$$V_{CM}^{+} = Z_{CM} \cdot I_{CM}^{+} \ . \tag{4}$$

For a pure DM signal arriving at the matched termination illustrated schematically in Fig. 2, the CM current and voltage are zero, and the DM current flows from one wire conductor to the other. This current flows through Z_3 and the series combination of Z_1 and Z_2, so the DM impedance is,

$$Z_{DM} = Z_3 \parallel (Z_1 + Z_2) \ . \tag{5}$$

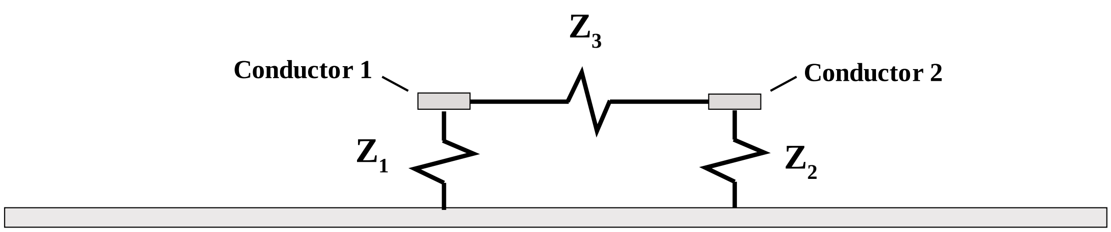

Fig. 2. A matched termination consisting of three resistances.

Combining (1), (3) and (5), we obtain the definition for I_{DM} necessary to ensure the independence of the DM and CM propagating modes,

$$I_{DM}^{+} = \frac{Z_1}{Z_1 + Z_2} \cdot I_1^{+} - \frac{Z_2}{Z_1 + Z_2} \cdot I_2^{+} \ . \tag{6}$$

For a pure CM signal arriving at the termination, the DM voltage and current are zero. Since both conductors have the same voltage, CM current flows from both conductors through the parallel combination of Z_1 and Z_2 to the reference conductor, so the CM impedance is,

$$Z_{CM} = Z_1 \parallel Z_2 \ . \tag{7}$$

Combining (2), (4) and (7) yields the definition for V_{CM},

$$V_{CM}^{+} = \frac{Z_2}{Z_1 + Z_2} V_1^{+} + \frac{Z_1}{Z_1 + Z_2} V_2^{+} \ . \tag{8}$$

For a backward propagating wave, we can define the DM and CM propagating modes similarly,

$$V_{DM}^{-} = V_1^{-} - V_2^{-} \tag{9}$$

$$I_{CM}^{-} = I_1^{-} + I_2^{-} \tag{10}$$

$$I_{DM}^{-} = \frac{Z_1}{Z_1+Z_2} \cdot I_1^{-} - \frac{Z_2}{Z_1+Z_2} \cdot I_2^{-} \tag{11}$$

$$V_{CM}^{-} = \frac{Z_2}{Z_1+Z_2} V_1^{-} + \frac{Z_1}{Z_1+Z_2} V_2^{-} \tag{12}$$

Combining both the forward and backward wave, i.e., combining (3), (4), (6) and (8) with the corresponding equations (9), (10), (11) and (12), we get,

$$V_{DM} = V_{DM}^{+} + V_{DM}^{-} = (V_1^{+} + V_1^{-}) - (V_2^{+} + V_2^{-}) = V_1 - V_2\sqrt{a^2+b^2} \ , \tag{13}$$

$$I_{CM} = I_{CM}^{+} - I_{CM}^{-} = (I_1^{+} - I_1^{-}) + (I_2^{+} - I_2^{-}) = I_1 + I_2 \ , \tag{14}$$

$$\begin{aligned} V_{CM} &= V_{CM}^{+} + V_{CM}^{-} \\ &= \frac{Z_2}{Z_1+Z_2}(V_1^{+} + V_1^{-}) + \frac{Z_1}{Z_1+Z_2}(V_1^{+} + V_1^{-}) \ , \\ &= \frac{Z_2}{Z_1+Z_2} V_1 + \frac{Z_1}{Z_1+Z_2} V_2 \end{aligned} \tag{15}$$

$$\begin{aligned} I_{DM} &= I_{DM}^{+} - I_{DM}^{-} \\ &= \frac{Z_1}{Z_1+Z_2}(I_1^{+} - I_1^{-}) - \frac{Z_1}{Z_1+Z_2}(I_2^{+} - I_2^{-}) \ . \\ &= \frac{Z_2}{Z_1+Z_2} I_1 - \frac{Z_1}{Z_1+Z_2} I_2 \end{aligned} \tag{16}$$

If we define

$$\frac{Z_2}{Z_1+Z_2} \equiv h \ , \tag{17}$$

then the DM and CM voltages and currents can be expressed as functions of V_1, V_2, I_1 and I_2 as follows,

$$V_{DM} = V_1 - V_2 \ , \tag{18}$$

$$I_{DM} = (1-h)I_1 - h \cdot I_2 \ , \tag{19}$$

$$V_{CM} = h \cdot V_1 + (1-h) \cdot V_2 \ , \tag{20}$$

$$I_{CM} = I_1 + I_2 \ . \tag{21}$$

This definition of common-mode and differential-mode voltage and current is consistent with that described by Uchida [21] and recent papers employing imbalance difference theory. The quantity, h, is called the *current division factor* or *imbalance factor*. Note that for a balanced transmission line, $Z_1 = Z_2$, and $h = 0.5$. In this case, (18)-(21) reduce to the familiar form for balanced TLs,

$$\begin{aligned} V_{DM} &= V_1 - V_2, \\ V_{CM} &= (V_1 + V_2)/2, \\ I_{DM} &= (I_1 - I_2)/2, \\ I_{CM} &= I_1 + I_2. \end{aligned} \tag{22}$$

3. Conversion between Differential Mode and Common Mode

By definition, as long as the electrical balance (defined by the quantity, h) does not change along the TL, the DM and CM signals propagate independently. However, as indicated by (19) and (20), any change in the electrical balance along the line will cause a discontinuity in the values of I_{DM} and V_{CM}. Fig. 3 shows a two-conductor TL above a reference plane that exhibits a change in the electrical balance. The matching impedances for the left section and right section of the TL are Z_{1L}, Z_{2L}, Z_{3L} and Z_{1R}, Z_{2R}, Z_{3R} respectively.

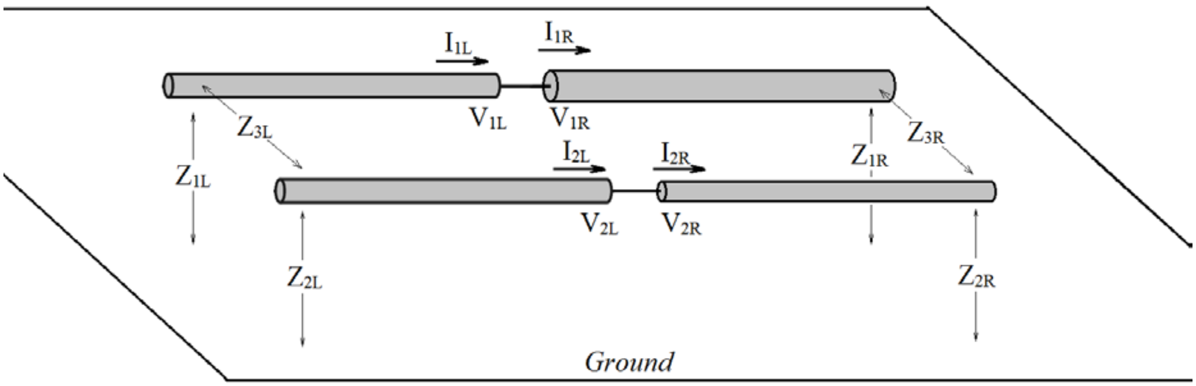

Fig. 3. TL with an electrical balance discontinuity above a reference plane.

At the interface where the electrical balance changes, the boundary conditions require the voltages and the currents on each conductor to be continuous, i.e.

$$\begin{aligned} V_{1L} &= V_{1R} \equiv V_1, \\ V_{2L} &= V_{2R} \equiv V_2, \\ I_{1L} &= I_{1R} \equiv I_1, \\ I_{2L} &= I_{2R} \equiv I_2. \end{aligned} \tag{23}$$

From (18) and (21), it is apparent that the DM voltage and CM current are also continuous at the interface,

$$V_{DM\_L} = V_1 - V_2 = V_{DM\_R} \equiv V_{DM} \ , \tag{24}$$

$$I_{CM\_L} = I_1 + I_2 = I_{CM\_R} \equiv I_{CM} \ . \tag{25}$$

The imbalance factors of the left section and right section are different,

$$h_L = \frac{Z_{2L}}{Z_{1L} + Z_{2L}} \ , \tag{26}$$

$$h_R = \frac{Z_{2R}}{Z_{1R} + Z_{2R}} \ . \tag{27}$$

Therefore, according to (19) and (20), the CM voltages and DM currents are different in the two sections of the TL,

$$
\begin{aligned}
V_{CM\_L} &= h_L \cdot V_1 + (1-h_L)\cdot V_2, \\
V_{CM\_R} &= h_R \cdot V_1 + (1-h_R)\cdot V_2, \\
I_{DM\_L} &= (1-h_L)I_1 - h_L \cdot I_2, \\
I_{DM\_R} &= (1-h_R)I_1 - h_R \cdot I_2.
\end{aligned} \tag{28}
$$

The change in the CM voltage and DM current across the interface can be expressed as,

$$\Delta V_{CM} = V_{CM\_L} - V_{CM\_R} = \Delta h \cdot (V_1 - V_2) = \Delta h \cdot V_{DM}\,, \tag{29}$$

$$\Delta I_{DM} = I_{DM\_L} - I_{DM\_R} = \Delta h \cdot (I_1 + I_2) = -\Delta h \cdot I_{CM}\,. \tag{30}$$

Equations (29) and (30) indicate that a change in the electrical balance along a transmission line results in a virtual CM voltage, ΔV_{CM}, that drives one side of the TL relative to the other side. ΔV_{CM} is proportional to the DM voltage at the interface and the change in the electrical balance. There will also be a virtual DM current, ΔI_{DM}, that flows from one conductor to the other at the interface. This DM current is virtual, because no actual electric charge moves from one conductor to the other. I_{DM} takes on a new value due to the fact that it is defined differently in terms of I_1 and I_2, which are constant across the interface. ΔI_{DM} is proportional to the CM current at the interface and the change in the electrical balance.

4. Models of the Differential Mode and Common Mode Conversion

For a two-conductor TL above a reference plane, we can decompose any signal into two independent propagating modes, DM and CM. In Fig. 4, the upper TL circuit represents only the DM propagation and the lower TL circuit represents only the CM propagation.

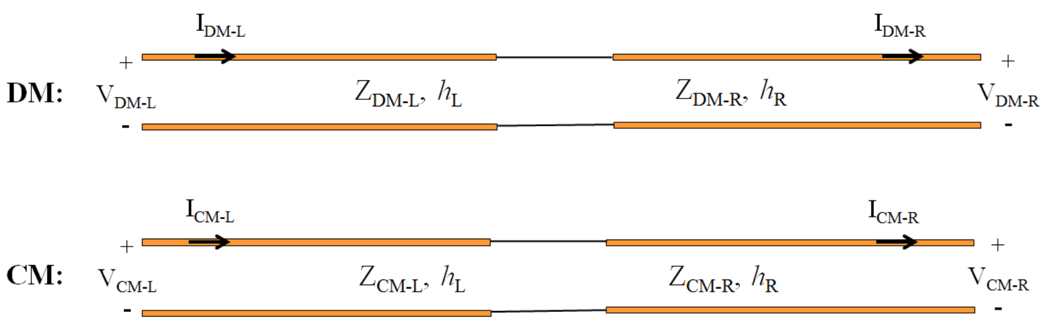

Fig. 4. Decomposition of the original circuit into DM and CM propagation.

4.1 Model of DM-to-CM Conversion

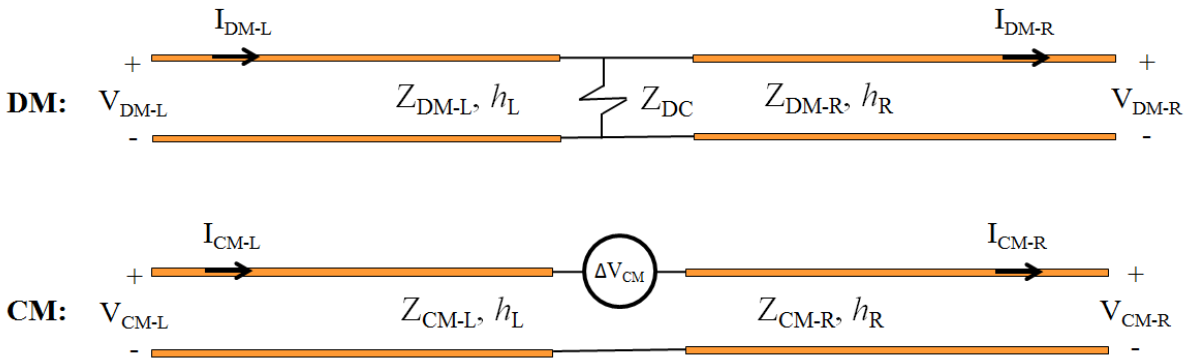

Fig. 5. Equivalent model for DM-to-CM conversion.

Consider a DM signal propagating on the DM TL of Fig. 4. From (29), it is clear that the DM voltage at the interface will generate a CM voltage difference, ΔV_{CM}. This can be represented as an ideal voltage source in the CM circuit as shown in the lower part of Fig. 5,

$$\Delta V_{CM} = V_{DM} \cdot \Delta h \ . \tag{31}$$

The ΔV_{CM} source will drive the CM circuit and generate a CM current, the impedance that ΔV_{CM} source sees is the series combination of the input impedances of each side of the TL in the CM circuit, so the generated CM current will be,

$$I_{CM} = \frac{\Delta V_{CM}}{Z_{CM-L} + Z_{CM-R}} = \frac{V_{DM} \cdot \Delta h}{Z_{CM-L} + Z_{CM-R}} . \tag{32}$$

According to (30), this I_{CM} at the interface will produce a DM current,

$$\Delta I_{DM} = \Delta h \cdot I_{CM} = \frac{V_{DM} \cdot (\Delta h)^2}{Z_{CM-L} + Z_{CM-R}} \ . \tag{33}$$

ΔI_{DM} can be regarded as the effect of the DM-CM conversion on the original DM signal. It can be represented by a shunt impedance in the DM circuit as shown in Fig. 5. Here, we will refer to it as the DM-to-CM conversion impedance,

$$Z_{DC} = \frac{V_{DM}}{\Delta I_{DM}} = \left(\frac{1}{\Delta h}\right)^2 \left[Z_{CM-L} + Z_{CM-R}\right]. \tag{34}$$

Z_{DC} is the loading effect on the DM signal that accounts for the energy conversion from DM to CM. If the coupling is weak (i.e. Δh is very small or the CM impedances are much bigger than the DM impedances), then Z_{DC} is much bigger than Z_{DM}, and it can be neglected. However, if the values of the CM impedances are comparable to the DM impedances and the change in electrical balance is significant, then Z_{DC} must be considered in order to accurately calculate the DM voltage at the interface.

4.2 Model of CM-to-DM Conversion

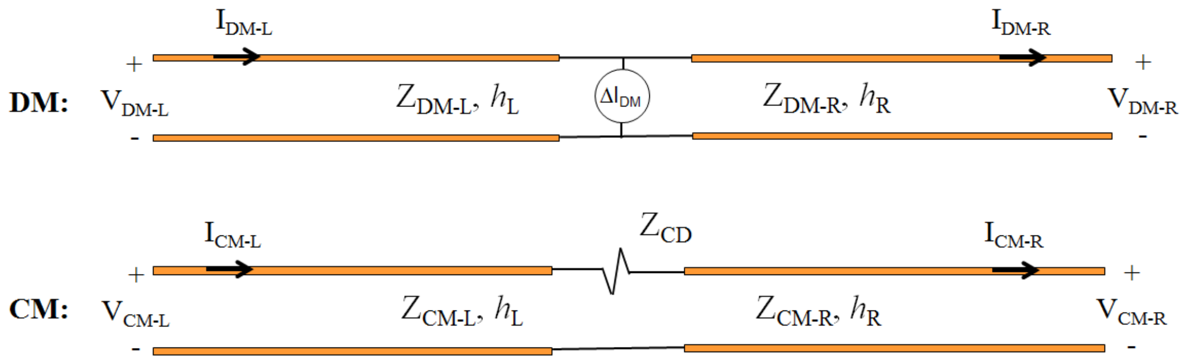

Fig. 6. Equivalent model for DM-to-CM conversion.

Equation (30) points out that CM current will generate DM current, ΔI_{DM}, at the interface where the electrical balance changes. This can be modeled as an ideal current source in the DM circuit, as shown in the upper part of Fig. 6,

$$\Delta I_{DM} = I_{CM} \cdot \Delta h . \tag{35}$$

In the DM circuit, ΔI_{DM} will flow through the parallel combination of the input impedances of both sides of the TL and generate a DM voltage at the interface:

$$V_{DM} = \Delta I_{DM} \cdot (Z_{DM-L} \,\|\, Z_{DM-R}) = I_{CM} \cdot \Delta h \cdot (Z_{DM-L} \,\|\, Z_{DM-R}) . \tag{36}$$

According to (29), this DM voltage will cause a change in CM voltage, ΔV_{CM}, at the interface,

$$\Delta V_{CM} = h \cdot V_{DM} = I_{CM} \cdot (\Delta h)^2 \cdot (Z_{DM-L} \,\|\, Z_{DM-R}) . \tag{37}$$

ΔV_{CM} can be regarded as the effect of the CM-DM conversion on the original CM circuit. It can be represented by a series impedance in the CM circuit, as shown in the lower part of Fig. 6. Here, it is referred to as the CM-DM conversion impedance,

$$Z_{CD} = \frac{\Delta V_{CM}}{I_{CM}} = (\Delta h)^2 \cdot (Z_{DM-L} \,\|\, Z_{DM-R}) . \tag{38}$$

Z_{CD} represents the loading effect on a CM signal that accounts for the energy conversion from CM to DM. Like Z_{DC}, Z_{CD} plays an important role if the two modes are strongly coupled, and it is negligible if the coupling is weak.

5. Example

This section demonstrates the implementation of these models on a multi-conductor transmission line structure where the coupling between the two modes is strong. As shown in Fig. 7, two cylindrical conductors of different radii form a two-conductor TL enclosed by a reference conductor. The total length of the TL is 600 mm. In the middle of the TL, the diameter of the two TL conductors abruptly changes, so that the electric balance is changed while the DM characteristic impedance stays the same. Near the left end of the TL, there is a 2-volt DM voltage source with 50-Ω internal impedance that drives the two conductors. The three-conductor system is perfectly matched at each end. The dimensions of the cross-section of the structure are shown in Fig. 8(a). The excitation frequency is 1GHz.

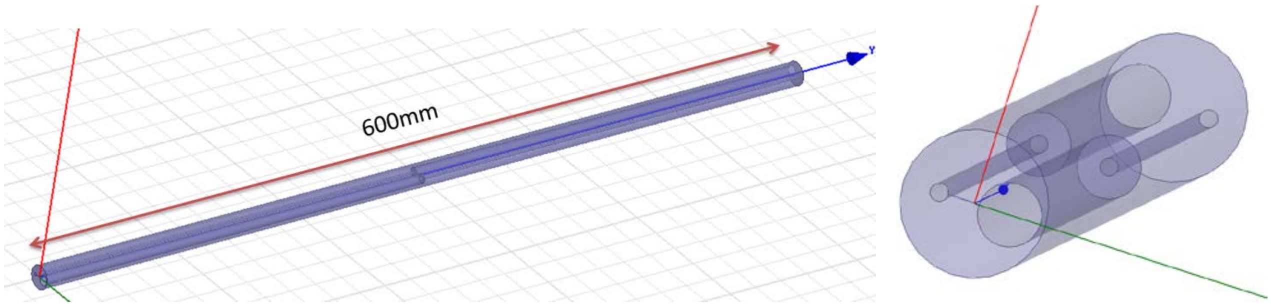

Fig. 7. The example structure.

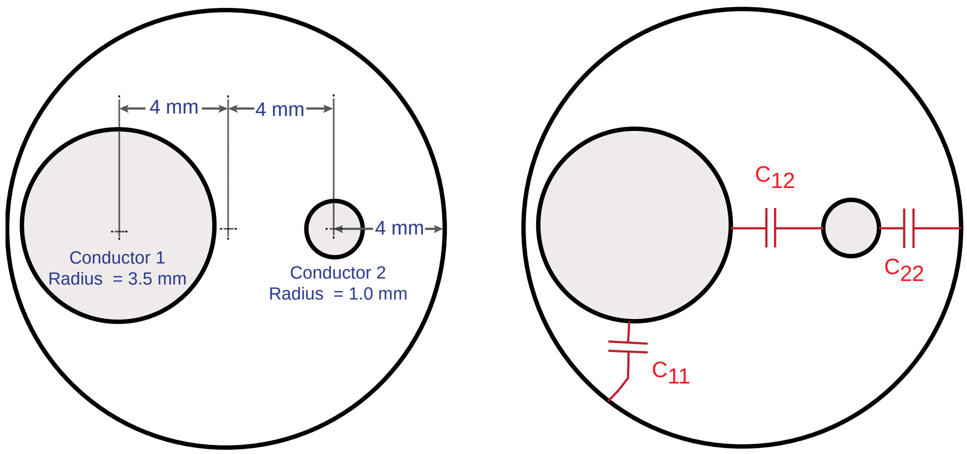

(a) Dimensions (b) Capacitances per unit length

Fig. 8. Cross-section of the transmission line in the example.

5.1 Calculation by Imbalance Difference Theory

The excitation is purely differential, but we expect to find power propagating in both modes due to the mode conversion that occurs at the middle of the line. To solve for the signal amplitudes in each mode using the imbalance difference theory, the imbalance factor on each side was calculated as a ratio of per-unit-length capacitances obtained using a 2D static field solver, ATLC2 [22]. The capacitances obtained are shown in Table I. The first three columns were obtained directly from the field solver. The values for C_{11}, C_{22} and C_{12} were obtained from the data in the first three columns. These capacitances are illustrated schematically in Fig. 8(b).

Table I. Capacitances calculated by ATLC2.

$C_{11}+C_{12}$	$C_{22}+C_{12}$	$C_{11}+C_{22}$	C_{11}	C_{22}	C_{12}
150.621 pF/m	33.91 pF/m	164.96 pF/m	140.84 pF/m	24.12 pF/m	9.78 pF/m

From the data in Table I, the imbalance factor of the two-conductor transmission line on one side of the discontinuity is,

$$h = \frac{C_{11}}{C_{11} + C_{22}} = 0.8538 . \tag{39}$$

On the other side of the discontinuity, because the conductors have a similar cross-section with positions of Conductor 1 and Conductor 2 switched, the imbalance factor is equal to one minus the imbalance factor on the first side. The change in the imbalance factor across the discontinuity is therefore,

$$\Delta h = h - (1 - h) = 0.7075 \,. \tag{40}$$

The per-unit-length capacitances associated with the DM and CM propagation are,

$$C_{DM} = C_{12} + C_{11} \cdot C_{22} / (C_{11} + C_{22}) = 30.38 \text{ pF/m} \,, \tag{41}$$

$$C_{CM} = C_{11} + C_{22} = 164.86 \text{ pF/m} \,. \tag{42}$$

Since both modes exhibit TEM propagation, the characteristic impedances of each mode are:

$$Z_{DM} = \frac{1}{u \cdot C_{DM}} = 109.7 \,\Omega \,, \tag{43}$$

$$Z_{CM} = \frac{1}{u \cdot C_{CM}} = 20.21 \,\Omega \,, \tag{44}$$

where u is the velocity of propagation. According to (34), the conversion impedance is,

$$Z_{DC} = \frac{V_{DM}}{\Delta I_{DM}} = \left(\frac{1}{\Delta h}\right)^2 \left[Z_{CM-L} + Z_{CM-R}\right] = 80.73 \,\Omega \,. \tag{45}$$

In the DM circuit as represented in Fig. 4, the impedance at the interface looking towards the right will be,

$$Z_{middle} = Z_{DC} \,||\, Z_{DM} = 45.51 \,\Omega \,. \tag{46}$$

The impedance at the source looking to the right will be,

$$Z_{source-right} = Z_{DM} \cdot \frac{Z_{middle} + j \cdot Z_{DM} \cdot \tan \beta l}{Z_{DM} + j \cdot Z_{middle} \cdot \tan \beta l} = 46.51 \,\Omega \,. \tag{47}$$

Therefore, the total impedance the DM source sees is,

$$Z_{input} = Z_{source-right} \,||\, Z_{DM} = 32.66 \,\Omega \,, \tag{48}$$

and the DM voltage across two conductors at the source is,

$$V_{DM@source} = V_{source} \cdot \frac{Z_{input}}{Z_s + Z_{input}} = 0.7903 \text{ V} \,. \tag{49}$$

At the interface, the voltage propagating towards the right (positive) direction will be,

$$V_0^+ = \frac{V_{DM@source}}{(e^{j\beta l} + \Gamma_{mid} \cdot e^{-j\beta l})} = 1.33 \text{ V} \,. \tag{50}$$

The reflection coefficient at the interface looking from the left is,

$$\Gamma_{middle} = \frac{Z_{middle} - Z_{DM}}{Z_{middle} + Z_{DM}} = -0.4046 \,. \tag{51}$$

So the DM voltage at the interface is,

$$V_{DM} = V^{+} + V^{+} \cdot \Gamma_{middle} = 0.79 \text{ V} . \quad (52)$$

Then from (31), the equivalent CM voltage source amplitude will be,

$$\Delta V_{CM} = V_{DM} \cdot \Delta h = 0.56 \text{ V} , \quad (53)$$

and the CM current will be,

$$I_{CM} = \frac{\Delta V_{CM}}{2 \cdot Z_{CM}} = 13.8 \text{ mA} . \quad (54)$$

Note that the left section of the TL is no longer impedance matched to the right section due to the mode conversion resistance. This will create a standing wave in the left section with standing wave ratio of,

$$SWR = \frac{1 + |\Gamma_{middle}|}{1 - |\Gamma_{middle}|} = 2.36 . \quad (55)$$

For the purpose of comparison, if we neglected to account for the conversion impedance in this example, then the DM voltage at the middle of the TL in Fig. 6 would have been the same as that at the source,

$$V_{DM}' = V_{source} \cdot \frac{Z_{DM} / 2}{Z_s + Z_{DM} / 2} = 1.046 \text{ V} . \quad (56)$$

In this case, the calculated CM current would have been,

$$I_{CM}' = \frac{\Delta V_{CM}}{2 \cdot Z_{CM}} = \frac{V_{DM} \cdot \Delta h}{2 \cdot Z_{CM}} = 18.3 \text{ mA} , \quad (57)$$

or 33% higher than the correct value.

5.2 Calculation by 3D full wave simulation

For validation purposes, the currents in the Fig. 7 structure were also calculated using a full wave simulation code, HFSS [23]. From these currents, the DM and CM currents were determined using (19) and (21). They are plotted in Fig. 9. The solid line is the CM current, which is constant along the TL. The dashed line is the DM current. It exhibits a standing wave pattern on the left half and is constant on the right. The CM current is about 13.3 mA, and the DM SWR is 2.34.

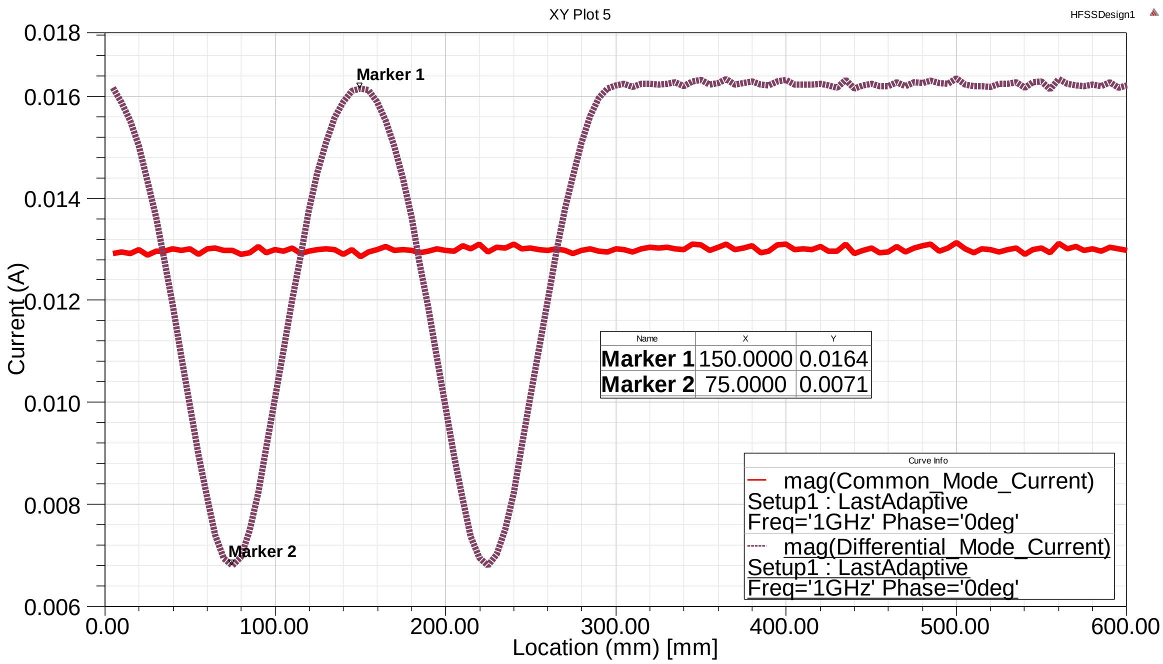

Fig. 9. HFSS calculation result.

Table II. Comparison of calculation result with different method.

Methods	Calculated CM current	SWR
Full wave simulation by HFSS	13.3 mA	2.34
TL model with conversion impedance	13.8 mA	2.36
TL model without conversion impedance	18.3 mA	N/A

Table II shows the calculated results from the full wave simulation, the TL model results with the modal conversion impedance, and the TL model results without accounting for the modal conversion impedance. There is good agreement (within 0.3 dB) between the TL result including the modal conversion impedance and the full wave simulation.

6. Conclusion

In a three-conductor transmission line, where one conductor is designated as the reference, the voltages and currents can be expressed in terms of orthogonal TEM DM and CM modes of propagation defined by (18)-(21). Any change in the electrical balance, as defined by (17), along the TL results in coupling between the DM and CM modes. A simple model describing DM-to-CM coupling consisting of an ideal source and conversion impedance was derived and is illustrated in Fig. 5. The change in the CM voltage at an interface is equal to the DM voltage at the interface times the change in the imbalance factor. This is true regardless of the whether the coupling between the two modes is weak or strong. The loading of the DM mode propagation can be modeled by a shunt resistor with the value calculated in (34).

A model describing the CM-to-DM coupling was also derived and is illustrated in Fig. 6. Whether the coupling is weak or strong, the change in the DM current at the interface is equal to the CM current at the interface times the change in the imbalance factor. The loading of the CM mode propagation can be modeled by a series resistor with the value provided in (38).

The conversion impedances have little impact on the calculated coupling if the converted power is a small percentage of the signal power (i.e. the coupling between the modes is weak). However, as the example in Section V demonstrates, the conversion impedance can have a significant effect on differential-mode signals when there is a large discontinuity in the balance, even when the characteristic impedance is maintained.

References

[1] G. I. Zysman and A. K. Johnson, "Coupled Transmission Line Networks in an Inhomogeneous Dielectric Medium," IEEE Trans. Microw. Theory Tech., vol. 17, no. 10, pp. 753–759, Oct. 1969.

[2] K. D. Marx, "Propagation Modes, Equivalent Circuits, and Characteristic Terminations for Multiconductor Transmission Lines with Inhomogeneous Dielectrics," IEEE Trans. Microw. Theory Tech., vol. 21, no. 7, pp. 450–457, Jul. 1973.

[3] V. K. Tripathi, "Asymmetric Coupled Transmission Lines in an Inhomogeneous Medium," IEEE Trans. Microw. Theory Tech., vol. 23, no. 9, pp. 734–739, Sep. 1975.

[4] G. I. Zysman and A. K. Johnson, "Coupled Transmission Line Networks in an Inhomogeneous Dielectric Medium," IEEE Trans. Microw. Theory Tech., vol. 17, no. 10, pp. 753–759, Oct. 1969.

[5] S. B. Cohn, "Shielded Coupled-Strip Transmission Line," IEEE Trans. Microw. Theory Tech., vol. 3, no. 5, pp. 29–38, Oct. 1955.

[6] R. A. Speciale, "Fundamental Even- and Odd-Mode Waves for Nonsymmetrical Coupled Lines in Non-Homogeneous Media," in S-MTT International Microwave Symposium Digest, 1974, vol. 74, no. 1, pp. 156–158.

[7] D. E. D. E. Bockelman, W. R. W. R. Eisenstadt, and S. Member, "Combined differential and common-mode scattering parameters: theory and simulation," IEEE Trans. Microw. Theory Tech., vol. 43, no. 7, pp. 1530–1539, Jul. 1995.

[8] Seungyong Baek, Seungyoung Ahn, Jongbae Park, Joungho Kim, Jonghoon Kim, and Jeong-hyeon Cho, "Accurate high frequency lossy model of differential signal line including mode-conversion and common-mode propagation effect," 2004 Int. Symp. Electromagn. Compat. (IEEE Cat. No.04CH37559), vol. 2, pp. 562–566, 2004.

[9] A. Sugiura and Y. Kami, "Generation and propagation of common-mode currents in a balanced two-conductor line," IEEE Trans. Electromagn. Compat., vol. 54, no. 2, pp. 466–473, Apr. 2012.

[10] F. Grassi, G. Spadacini, and S. A. Pignari, "The Concept of Weak Imbalance and Its Role in the Emissions and Immunity of Differential Lines," IEEE Trans. Electromagn. Compat., vol. 55, no. 6, pp. 1346-1349, Dec. 2013.

[11] F. Grassi, Y. Yang, X. Wu, G. Spadacini and S. A. Pignari, "On mode conversion in geometrically unbalanced differential lines and its analogy with crosstalk," IEEE Trans. Electromagn. Compat., vol. PP, no.99, pp.1-9, doi: 10.1109/TEMC.2014.2372894.

[12] K. Sejima, Y. Toyota, K. Iokibe, L.R. Koga, and T. Watanabe, "Experimental model validation of mode-conversion sources introduced to modal equivalent circuit," 2012 IEEE International Symposium on Electromagnetic Compatibility, pp.492-497, Aug. 2012.

[13] Y. Toyota, K. Iokibe, and L. R. Koga, "Mode conversion caused by discontinuity in transmission line: From viewpoint of imbalance factor and modal characteristic impedance," in 2013 IEEE Electrical Design of Advanced Packaging Systems Symposium (EDAPS), pp. 52-55, 2013.

[14] T. Watanabe, O. Wada, T. Miyashita, and R. Koga, “Common-mode-current generation caused by difference of unbalance of transmission lines on a printed circuit board with narrow ground pattern,” IEICE Trans. Commun., vol. E83-B, no. 3, pp. 593–599, Mar. 2000.

[15] T. Watanabe, H. Fujihara, O. Wada, R. Koga, and Y. Kami, “A prediction method of common-mode excitation on a printed circuit board having a signal trace near the ground edge,” IEICE Trans. Commun., vol. E87-B, no. 8, pp. 2327–2334, Aug. 2004.

[16] O. Wada, “Modeling and simulation of unintended electromagnetic emission from digital circuits,” Electron. Commun. Japan (Part I Commun., vol. 87, no. 8, pp. 38–46, Aug. 2004.

[17] T. Matsushima, T. Watanabe, Y. Toyota, R. Koga, and O. Wada, “Evaluation of EMI reduction effect of guard traces based on imbalance difference model,” IEICE Trans. Commun., vol. E92-B, no. 6, pp. 2193–2200, Jun. 2009.

[18] Y. Kayano, K. Mimura, and H. Inoue, “Evaluation of imbalance component and EM radiation generated by an asymmetrical differential-paired lines structure,” Trans. JIEP, vol. 4, no.1, pp. 6-16, Dec. 2011.

[19] C. Su and T. H. Hubing, “Imbalance difference model for common-mode radiation from printed circuit boards,” IEEE Trans. Electromagn. Compat., vol. 53, no. 1, pp. 150–156, Feb. 2011.

[20] H. Kwak and T. H. Hubing, “Investigation of the imbalance difference model and its application to various circuit board and cable geometries,” 2012 IEEE International Symposium on Electromagnetic Compatibility, 2012, pp. 273–278.

[21] H. Uchida, Fundamentals of Coupled Lines and Multiwire Antennas, Sasaki Printing and Publishing, pp. 37-39, 1967.

[22] “atlc2 - Arbitrary Transmission Line Calculator.” [Online]. Available: http://www.hdtvprimer.com/KQ6QV/atlc2.html. [Accessed: 12-Aug-2014].

[23] “ANSYS HFSS,” [Online]. Available: http://www.ansys.com/Products/Simulation+Technology/Electronics/Signal+Integrity/ANSYS+HFSS. [Accessed: 20-Aug-2014].